Contract No:

This document was prepared in conjunction with work accomplished under Contract No. DE-AC09-08SR22470 with the U.S. Department of Energy.

Disclaimer:

TRITIUM AGING EFFECTS ON THE FRACTURE TOUGHNESS PROPERTIES OF STAINLESS STEEL BASE METAL AND WELDS

Michael J. Morgan
Savannah River National Laboratory, Aiken, SC
SRNL-STI-2009-00475

Introduction

Tritium reservoirs are constructed from welded stainless steel forgings. While these steels are highly resistant to the embrittling effects of hydrogen isotopes and helium from tritium decay; they are not immune (1-4). Tritium embrittlement is an enhanced form of hydrogen embrittlement because of the presence of helium-3 from tritium decay which nucleates as nanometer-sized bubbles on dislocations, grain boundaries, and other microstructural defects. Steels with decay helium bubble microstructures are hardened and less able to deform plastically and become more susceptible to embrittlement by hydrogen and its isotopes (1-4). Ductility, elongation-to-failure, and fracture toughness are reduced by exposures to tritium and the reductions increase with time as helium-3 builds into the material from tritium permeation and radioactive decay (3, 4).

Material and forging specifications have been developed for optimal material compatibility with tritium. These specifications cover composition, mechanical properties, and select microstructural characteristics like grain size, flow-line orientation, inclusion content, and ferrite distribution. For many years, the forming process of choice for reservoir manufacturing was high-energy-rate forging (HERF), principally because the DOE forging facility owned only HERF hammers. Today, some reservoir forgings are being made that use a conventional, more common process known as press forging (PF or CF) (5). One of the chief differences between the two forging processes is strain rate: Conventional hydraulic or mechanical forging presses deform the metal at 4-8 ft/s, about ten-fold slower than the HERF process. The material specifications continue to provide successful stockpile performance by ensuring that the two forging processes produce similar reservoir microstructures. While long-term life storage tests have demonstrated the general tritium compatibility of tritium reservoirs, fracture-toughness properties of both conventionally forged and high-energy-rate forged are needed for designing and establishing longer tritium-reservoir lifetimes, ranking materials, and, potentially, for qualifying new forging vendors or processes. Measurements on the effects of tritium and decay helium on the fracture toughness properties of CF stainless steels having similar composition, grain size, and mechanical properties to previously studied HERF steels are needed and have not been conducted until now.

The compatibility of stainless steel welds with tritium represents another concern for long-term reservoir performance. Weldments have not been well-characterized with respect to tritium embrittlement, although a recent study was completed on the effect of tritium and decay helium on the fracture toughness properties of Type 304L weldments (6-8). This study expands the characterization of weldments through measurements of tritium and decay helium effects on the fracture toughness properties of Type 21-6-9 stainless steel.

The purpose of this study was to measure and compare the fracture toughness properties of Type 21-6-9 stainless steel for conventional forgings and weldments in the non-charged, hydrogen-charged and tritium-charged-and-aged conditions.

Experimental

Fracture toughness samples (Fig. 1) were fabricated from base metals and weldments of Type 21-6-9 Stainless Steel. The compositions of the steels and weld filler metals used in the study are listed in Table I and their yield strengths are given in Table II. The base metal was supplied in the form of forward extruded cylindrical conventional or high-energy-rate forgings. The two forging processes are described by Robinson (5). For a select number of forgings, notched groves were cut along the length of the forgings and the grooves were filled using the Gas Tungsten Arc (GTA) welding process and Type 308L filler wire. After welding, the forgings were sectioned into round discs and radiographed to verify that there was no unusual porosity, cracks, or other macroscopic defects from the welding process. This was done to ensure the fracture- toughness samples were machined from high-quality welds and that any differences in properties could be attributed to the weldment microstructure. Arc-shaped fracture-mechanics specimens having the shape and dimensions shown in Fig. 1 were fabricated from the perimeter of each disc and fatigue-cracked so that the crack-length to sample-width ratio was between 0.4 and 0.6. For the base metals, the crack face was parallel to the forging direction and ran from the center of the forging toward the outer perimeter. For welds, the crack propagation was along the weld centerline and directed away from the base of the weld.

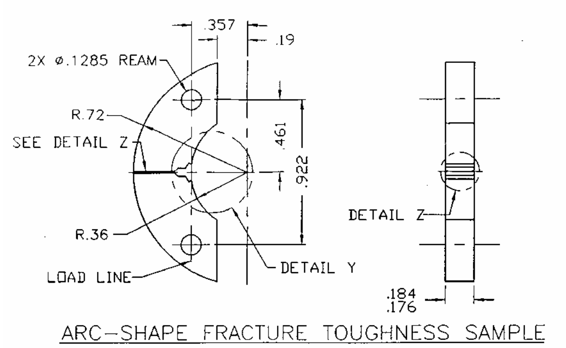

Fig. 1. Shape and Dimensions of Fracture-Toughness Sample. Dimensions shown are in Inches.

Table I. Compositions Stainless Steel Forgings, Plates and Weld Filler Wires (Weight %)

Material	Cr	Ni	Mn	Mo	C	Si	Cu	P	S	N	Co	O	Al
308L Filler Wire	20.5	10.3	1.56	<0.01	0.028	0.5	0.015	0.006	0.012	0.055	0.068	-	-
21-6-9 HERF	19.4	6.4	8.5	.-	.04	.33	-	.021	<.001	.28	-	.002	<.001
21-6-9 CF HT-1	19.1	6.7	9.9	-	.03	.41	-	.01	.004	.28	-	.001	.005
21-6-9 CF HT-2	19.3	6.7	9.9	-	.03	.38	-	.01	.001	.28	-	.002	.004

Notes:

308L Filler wire and HERF Steel used for Type 21-6-9 weldments
CF – Conventional Forging
HERF – High-energy-rate Forging

Table II. Materials and Yield Strengths

Material	Yield Strength (MPa)
308L Filler Wire	Not Meas.
21-6-9 HERF	722
21-6-9 CF Heat I	600
21-6-9 CF Heat 2	685

Typical microstructures of the Type 21-6-9 base metal and weldments are shown in Fig. 2. The base metal microstructures of consisted of austenite with grains elongated in the direction of forging while the weldment microstructures consisted of discontinuous skeletal and lathy ferrite in a predominant austenite matrix.

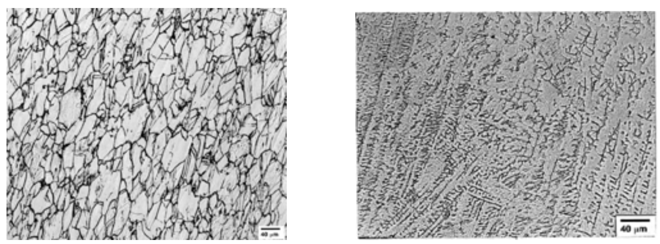

(a) (b)

Fig. 2. Microstructures of Type 21-6-9 Stainless Steel: (a) Forged Base Metal and (b) Weld Metal

Non-charged samples were tested in air at ambient temperature in the as-forged and as-welded conditions. Companion samples were charged with either hydrogen or tritium gas at 623 K and an over-pressure of 34.5 MPa or 69 MPa and then stored in air at 223 K. The temperature of exposure was designed to uniformly saturate the samples with hydrogen or tritium without changing the steel microstructure; the storage temperature was designed to minimize tritium off-gassing and allow for the build-in of helium from tritium decay until testing was performed. Testing of the tritium-charged samples was conducted over a period of years to measure the effect of decay helium content on the fracture-toughness properties. After testing, the helium content of selected tritium-charged samples was determined by isotope-dilution gas mass spectrometry following vaporization in a resistance-heated graphite crucible. The amount of helium in each sample was back-calculated to the test date from the measured helium contents.

J-integral tests were conducted at room temperature in air using a screw-driven testing machine and a crosshead speed of 0.002 mm/s while recording load, load-line displacement with a gage clipped to the crack mouth, and crack length. Crack length was monitored using an alternating DC potential drop system and guidelines described in ASTM E647-95 (9). The J-Integral versus crack length increase curves (J-R curves) were constructed from the data using ASTM E1820-99 (10). The material fracture toughness value, J_Q, was obtained from the intercept of an offset from the crack tip blunting line with the J-R curve. The samples were thick enough to maintain flat fracture and thin enough so that uniform initial hydrogen or tritium concentrations could be achieved without changing material microstructures during charging.

Results and Discussion

Typical J-R curves for the non-charged base metals and weldments of Type 21-6-9 stainless steel (this study) are shown in Fig. 3 along with the J-R curves for Type 304L stainless steel from the earlier study (6). The fracture toughness value, $J_{Q,}$ was determined from the intercept of an 0.2 mm offset line with the J-R curve (10). For both studies, the weldments have an average J_Q fracture-toughness value two-to-three times higher than the base metal values. The high weldment fracture toughness was attributed to the presence of a ductile delta-ferrite phase (5-8% by volume) in the predominant austenite microstructure (6, 11). The resistance to continued crack propagation was also improved in weldments over base metals, and is indicated by the steep-sloped J-R curves of the weldments compared to the shallow-sloped J-R curves for base metals in Fig. 3.

Hydrogen charging lowered the resistance of the Type 21-6-9 base metal to crack initiation and growth as indicated by the lower J_Q values and the less-steep J-R curves in Fig 4. The effect was even greater as the charging pressure was increased from 34.5 MPa to 69 MPa.

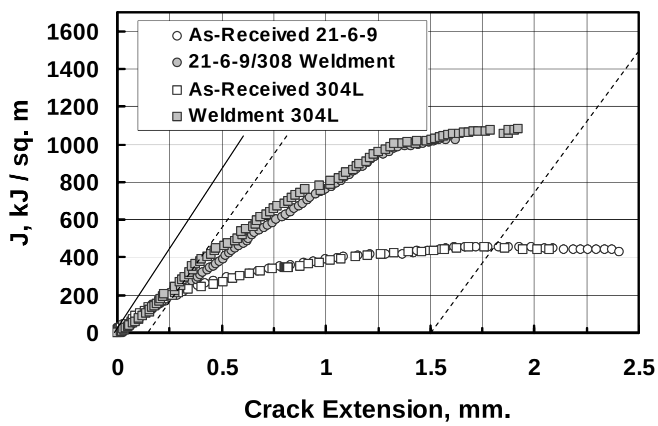

Fig. 3. J-R Behavior for Base Metals and Weldments of Types 304L and 21-6-9 Stainless Steels.

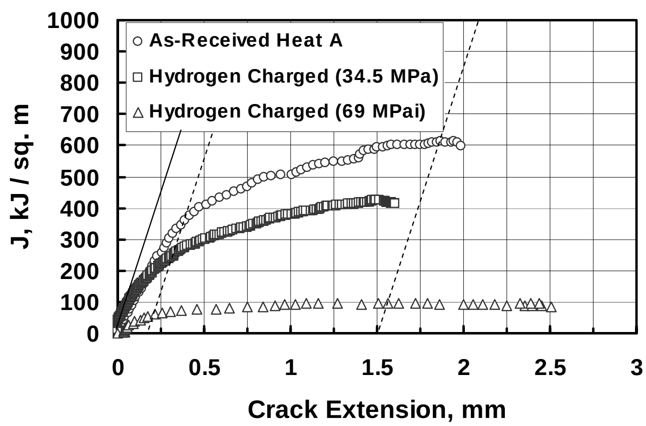

Fig. 4. Effect of Hydrogen on J-R Behavior of Type 21-6-9 Stainless Steel Base Metals.

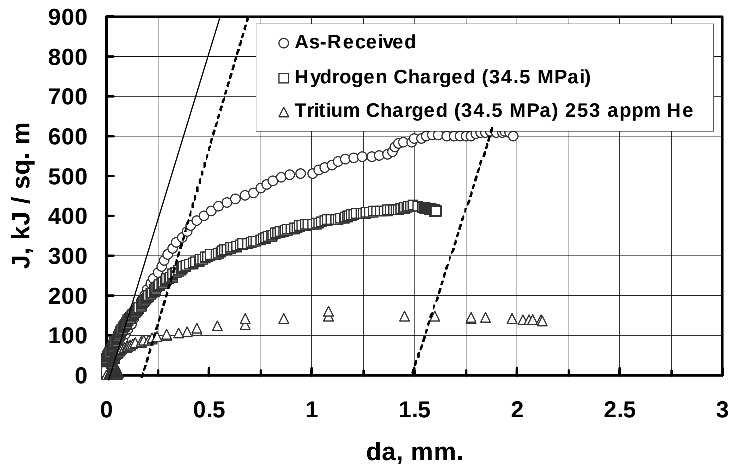

Fig. 5. J-R Behavior for Non-Charged (As-Received), Hydrogen-Charged and Tritium-Charged-and-Aged Type 21-6-9 Stainless Steel Base Metals

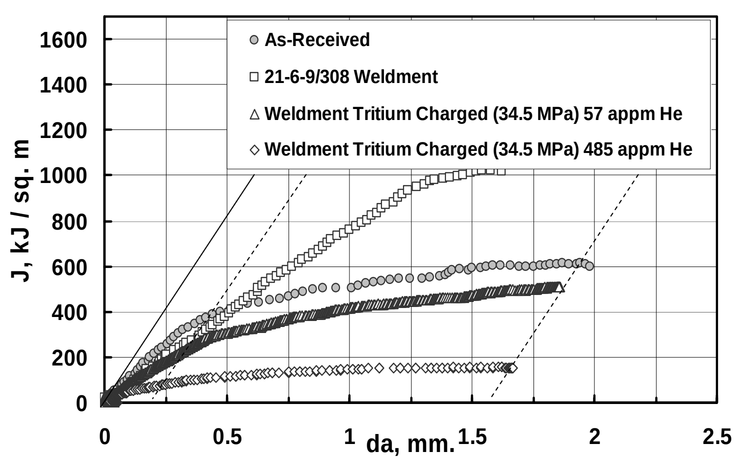

Fig. 6. J-R Behavior for Non-Charged (As-Received), Hydrogen-Charged and Tritium-Charged-and-Aged Type 21-6-9 Stainless Steel Weldments

The effect of tritium exposure on the J-R behavior of Type 21-6-9 stainless steel base metals is shown in Fig. 5. Tritium-charged samples had lower fracture toughness than samples similarly charged with hydrogen because of the presence of helium from tritium decay. Hydrogen-and tritium-charged base metals had facture surfaces that were different than non-charged steels (11). Fracture occurred by microvoid nucleation and growth but the microvoids had a much smaller size and finer spacing than what was observed on the non-charged fractures (11).

Tritium and decay helium had a remarkable effect on base metal and weldment toughness, as shown in Fig.6. Note the large reduction in fracture toughness with increasing helium content. Cracking along ferrite/austenite interfaces or through the ferrite was observed on the weldment fracture surfaces after tritium exposure (6, 11). Furthermore, for base metals and weldments, the J_Q fracture toughness values decreased further with increasing decay helium content (Fig. 7).

After helium builds in from tritium decay the initially high weldment fracture toughness is reduced to values similar to the tritium-charged base metal values (Fig. 7).

The effect of ferrite on weldment toughness for non-charged steels is in agreement with that described in other studies (12-14). Brooks (12) points out that the ductile ferrite phase tends to blunt propagating cracks and provides a tortuous path through the microstructure of weldment while Mills (13) indicates that ferrite phases in stainless steel weldments are brittle at low temperature and welds exhibit a ductile-brittle transition temperature phenomenon. At ambient and elevated temperatures, Mills shows that the ferrite phase behaves in a ductile manner, and welds are more resistant to fracture (13).

For charged steels, the weldments toughness behavior seen in this study is consistent with the fracture process that Mills describes except that the ferrite phase is embrittled by tritium and helium. The fracture modes of weldments appear to be consistent with Brooks (14) in that hydrogen-induced fracture occurs along or near the austenite-ferrite boundary in welds although more work is needed to confirm this.

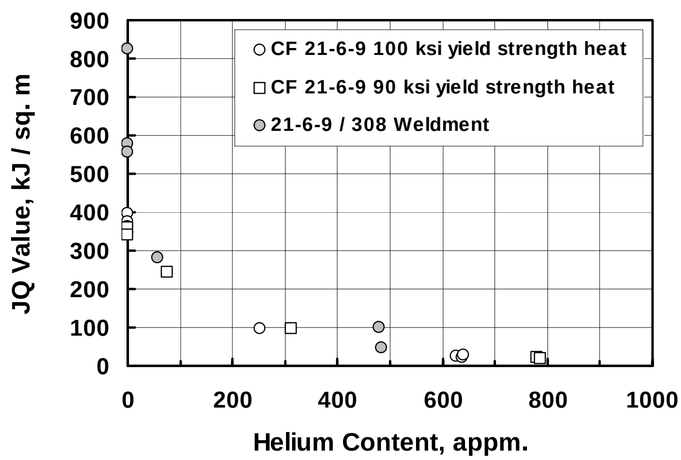

(b)

Fig. 7. Effect of Decay Helium Content on the J_Q Value of Type 21-6-9 Stainless Steel and its Weldment

Conclusions

[1]. For Type 21-6-9 stainless steel, the fracture toughness of weldments is two to three times higher than the base-metal toughness. The toughness improvement is attributed to the ductile ferrite phase in the predominant austenite microstructure.

[2]. Hydrogen and tritium exposure lowered the fracture-toughness properties of both base metals and weldments to similar values. Toughness decreased with increasing helium content from tritium decay.

[3]. The percent reduction in weldment toughness was more severe than the reduction in base-metal toughness because of hydrogen and tritium embrittlement of the weld-ferrite phase.

Acknowledgements

The author would like to thank Scott West and Glen Chapman for their assistance in producing the weldments and testing the samples for this study.

References

[1]. G. R. Caskey, Jr., "Hydrogen Effects in Stainless Steels", Hydrogen Degradation of Ferrous Alloys, J. P. Hirth, R. W. Oriani, and M. Smialowski, eds., Noyes Publication, Park Ridge, NJ, 1985, p. 822.

[2]. G. R. Caskey, Jr., "Tritium-Helium Effects in Metals", Fusion Technology, Vol. 8, 1985, pp. 2293-2298.

[3]. M. J. Morgan and M. H. Tosten, "Tritium and Decay Helium Effects on the Fracture Toughness Properties of Types 316L, 304L, and 21Cr-6Ni-9Mn Stainless Steels", Hydrogen Effects in Materials, ed. A. W. Thompson and N. R. Moody, (Warrendale, PA: TMS, 1996), p. 873.

[4]. S. L. Robinson, "The Effects of Tritium on The Flow and Fracture of Austenitic Stainless Steels", Proc. Fourth Int. Conf. on Hydrogen Effects on Material Behavior, A. W. Thompson and N. R. Moody, eds., The Minerals, Metals & Materials Society, Warrendale, PA, 1989, p. 433.

[5]. S. L. Robinson, B. C. Odegard, Jr., N. Y.C. Yang, D. A. Hughes, and T. Headley, "Analysis of the Microstructure and Suitability of the First Commercial Forgings for Gas Transfer System Applications", SANDIA Report SAND99-8243, October, 1999.

[6]. M. J. Morgan, M. H. Tosten, and S. L. West, "Tritium Effects on Weldment Fracture Toughness", Savannah River National Laboratory, WSRC-STI—2006-00056, July 17 2006.

[7]. M. H. Tosten and M. J. Morgan, "Microstructural Study of Fusion Welds in 304L and 21Cr-6Ni-9Mn Stainless Steels (U)", WSRC-TR-2004-00456, March, 2005

[8]. M. H. Tosten and M. J. Morgan, "Transmission Electron Microscopy Study of Helium-Bearing Fusion Welds", WSRC-TR-2005-00477, November, 2005.

[9]. ASTM E647-95a "Standard Test Method for Measurement of Fatigue Crack Growth Rates" "1999 Annual Book of ASTM Standard Volume 3.01 Metals-Mechanical Testing; Elevated and Low-Temperature Tests; Metallography, American Society for Testing and Materials, 1999.

[10]. ASTM E1820-99 "Standard Test Method for Measurement of Fracture Toughness", 1999 Annual Book of ASTM Standard Volume 3.01 Metals-Mechanical Testing; Elevated and Low-Temperature Tests; Metallography, American Society for Testing and Materials, 1999.

[11]. M. J. Morgan, S. L. West, and G. K. Chapman, "Tritium Aging Effects on Fracture Toughness of Type 21-6-9 Stainless Steel", Savannah River National Laboratory, WSRC-STI-2007-00244, June 14, 2007.

[12]. J. A. Brooks, A. W. Thompson, and J. C. Williams, "A Fundamental Study of the Beneficial Effects of Delta Ferrite in Reducing Weld Cracking", Welding Journal, Vol. 63, No. 3 (1984), 71s-80s.

[13]. W. J. Mills, "Fracture Toughness of Type 304 and 316 Stainless Steels and Their Welds", International Materials Reviews, 42 (2) (1997), 45-82.

[14]. J. A. Brooks and A. J. West, "Hydrogen Induced Ductility Losses in Austenitic Stainless Steel Welds", Metallurgical Transactions A, 12A, (1981) 213-223.